Avalanche photodetector in the GaSb/AlSb/InAs material system by molecular beam epitaxy

Xiao-Chang Cheng, Thomas C. McGill

Xiao-Chang Cheng, Thomas C. McGill, "Avalanche photodetector in the GaSb/AlSb/InAs material system by molecular beam epitaxy," Proc. SPIE 3629, Photodetectors: Materials and Devices IV, (7 April 1999); doi: 10.1117/12.344563

SPIE.

Event: Optoelectronics '99 - Integrated Optoelectronic Devices, 1999, San Jose, CA, United States

Avalanche photodetector in the GaSb/AlSb/InAs material system by molecular beam epitaxy

X-C. Cheng and T. C. McGill

Department of Applied Physics, California Institute of Technology, Pasadena, CA 91125

ABSTRACT

GaSb/AlSb/InAs is an attractive system for making low noise avalanche photodetectors (APD) due to possible resonant enhancement of hole impact ionization in $Al_xGa_{1-x}Sb$ and potential enhancement of electron impact ionization in GaSb/AlSb superlattices. We have employed molecular beam epitaxy (MBE) to fabricate device structures so that these effects could be further explored. The devices were grown on GaSb substrates and incorporated a p^-n^+ one sided abrupt junction. The p^- multiplication region consisted of either bulk $Al_{0.04}Ga_{0.96}Sb$ or 10 periods of alternating, 300 Å thick GaSb and AlSb layers. A short period, selectively doped InAs/AlSb superlattice was used as the n^+ layer. Dark current suppression in these devices was found to be largely dependent on the InAs/AlSb superlattice configuration and the resulting band offset at the p^-n^+ heterojunction. Notably, for devices with a 0.6 μm $Al_{0.04}Ga_{0.96}Sb$ multiplication region and an optimized InAs/AlSb superlattice, an avalanche break down voltage of 13 V was observed. The dark current density for this device was 6 A/cm^2 at a multiplication factor of 10. Devices with GaSb/AlSb superlattice multiplication regions exhibited a higher breakdown voltage (18.5 V) and a lower dark current density (0.4 A/cm^2) at comparable gain. Impact ionization rates in $Al_{0.04}Ga_{0.96}Sb$ were studied by using 781 nm and 1645 nm laser light. The results were consistent with enhancement of hole impact ionization in $Al_{0.04}Ga_{0.96}Sb$.

Keywords: Avalanche photodetector, Molecular beam epitaxy, AlGaSb, Superlattice, Dark current, Impact ionization,

1. INTRODUCTION

The 6.1 Å lattice matched system formed by GaSb, AlSb and InAs has many possibilities in device application due to the unique type II band alignment between these materials and the wide range of bandgaps available. Optical devices in the near and far infrared including cascade lasers,[1] injection lasers[2] and superlattice detectors[3] have already been reported. There is much interest in making an avalanche photodetector (APD) in this material system. An APD employing GaSb as the absorption region has responsivity in the near infrared up to 1.7 μm, and has potential applications in optical communication, gas sensing and night vision. In addition to expanding the integration capability of the material system, antimonide APD's have some intrinsic advantages: the carrier impact ionization rates of GaSb are larger than those of InP,[4] which leads to shorter avalanche regions compatible with high speed operation. The antimonide system also provides unique possibilities for enhancement of either hole or electron impact ionization, which is the prerequisite for making devices with low excess noise factor and high gain-bandwidth product.[5]

The hole to electron impact ionization ratio (K_p/K_n) in $Al_xGa_{1-x}Sb$ is thought to be enhanced near $x = 0.06$ where the spin-orbit split-off band offset Δ matches the band gap energy. The effect is attributed to lowering of the hole ionization energy and was first demonstrated experimentally by Hildebrand et al.[6] However, other experimental and theoretical studies have since generated contradictory results. In particular, Hidelbrand's findings were supported by Gouskov et al.[7] whereas Kuwatsuka et al.[8] showed that K_p/K_n in $Al_{0.06}Ga_{0.94}Sb$ was lower than previously measured and there was no enhancement of K_p/K_n at the split-off band resonant condition. The aforementioned studies have all used liquid phase epitaxy (LPE) as the crystal growth method. Since the effect is possibly material dependent,[9] new insights may be obtained by studying similar device structures fabricated from molecular beam epitaxy.

The composition and thickness control inherent to MBE can also be utilized to achieve high K_n/K_p by using a GaSb/AlSb superlattice as the multiplication layer. Electrons will preferentially impact ionize in the superlattice

Correspondence: E-mail: xcc@ssdp.caltech.edu; Telephone: 626 395 2133; Fax 626 395 4817

Part of the SPIE Conference on Photodetectors: Materials and Devices IV
San Jose, California • January 1999
SPIE Vol. 3629 • 0277-786X/99/$10.00

if the conduction band offset between the constituent materials is larger than their valence band offset.[10] This effect has been demonstrated in GaAs/AlAs and InGaAs/InAlAs superlattices by a number of workers.[11,12] But the scheme has not been adequately exploited in the GaSb/$Al_xGa_{1-x}Sb$ system despite the large band offset differences available.

In this paper, we have attempted to use MBE to fabricate antimonide APD's using both GaSb/AlSb superlattices and bulk $Al_{0.04}Ga_{0.96}Sb$ as the multiplication layer. The flexibility of the MBE technique was demonstrated by the use of an InAs/AlSb superlattice as the device n-type layer and the incorporation of both multiplication layer designs in the same basic structure. Dark current and photo gain characteristics of these devices were analyzed to establish performance limits on the two types of structures. Photo response measurements employing 781 nm and 1645 nm lasers were also carried out to explore possible resonant enhancement of hole impact ionization in $Al_{0.04}Ga_{0.96}Sb$.

2. DEVICE DESIGN

The basic device structure employed in this study is shown in Fig. 1 and comprised of three sections: a heavily doped p^+ GaSb layer ($p=2\times10^{18}/cm^3$) for bottom contact, an unintentionally dope p^- region, and a heavily doped n^+ InAs/AlSb superlattice ($n=1\times10^{18}/cm^3$). Avalanche multiplication took place in the p^- layer, which consisted of either bulk $Al_xGa_{1-x}Sb$ or a GaSb/AlSb superlattice. Four samples were fabricated and examined in detail in this study. The exact structures of these samples are listed in Table 1.

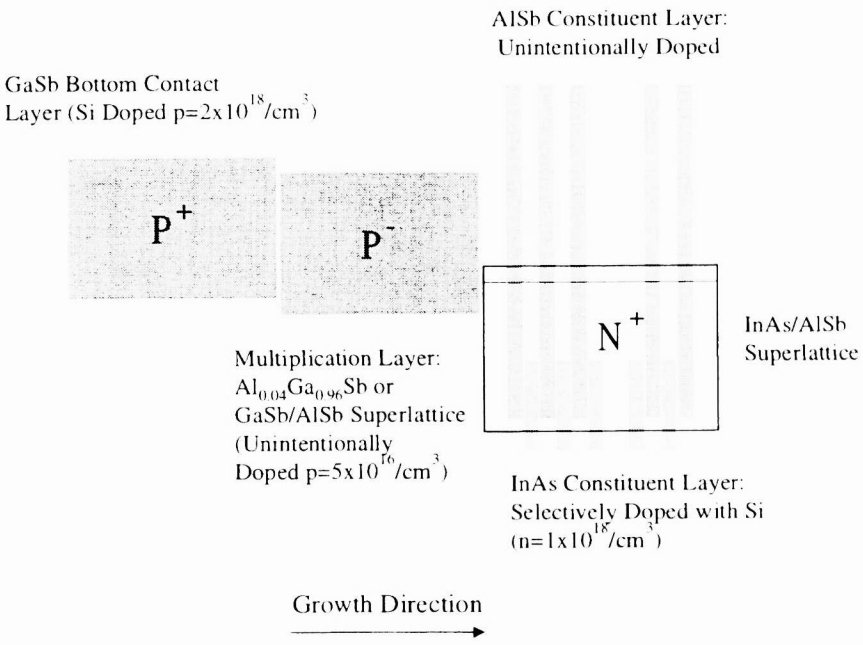

Figure 1. Basic structure and band alignment of the antimonide APD. The device had a p^-n^+ configuration with p^- $Al_{0.04}Ga_{0.96}Sb$ or GaSb/AlSb superlattice multiplication layers and a n^+ selectively doped InAs/AlSb superlattice.

The Al concentration in the multiplication region of bulk devices was kept at 0.04, which was near the composition for spin-orbit split-off band resonance. Due to the low vapor pressure of Sb, Ga atoms tend to occupy Sb sites during crystal growth of $Al_xGa_{1-x}Sb$ and form defects which are double acceptors. Thus unintentionally doped $Al_xGa_{1-x}Sb$ is always p-type. Hall experiment on calibration samples grown in our MBE system yielded a background doping of $5\times10^{16}/cm^3$ for the p^- multiplication layer. Given the bandgap of $Al_{0.04}Ga_{0.96}Sb$ at 0.75 eV, and an one sided abrupt pn junction at such a doping level, the device was estimated to have an avalanche breakdown voltage of 14 V.[13] The depletion width on the lightly doped side was estimated to be 0.6 μm at breakdown. Thus the $Al_{0.04}Ga_{0.96}Sb$ multiplication layer was kept to be at least 0.6 μm thick to maximize the length of the multiplication region.

The multiplication region of the superlattice device consisted of 10 periods of alternating GaSb and AlSb layers. GaSb and AlSb were selected as the superlattice components because of the large conduction band offset (1.1 eV to

Table 1. List of APD structures fabricated. APD's with $Al_{0.04}Ga_{0.96}Sb$ as the multiplication layer were fabricated with three different InAs/AlSb superlattice configurations to optimize dark current suppression and improve contact resistance.

Sample Number	p^- Multiplication Layer	n^+ InAs/AlSb Superlattice
754	1 μm, $Al_xGa_{1-x}Sb$	0.5 μm, 27 Å / 27 Å
757	0.6 μm, $Al_xGa_{1-x}Sb$	0.3 μm, 10 Å / 20 Å
759	0.6 μm, $Al_xGa_{1-x}Sb$	300 Å , 5 Å / 10 Å layer, followed by 0.2 μm, 10 Å / 20 Å layer, followed by 0.1 μm, 27 Å / 27 Å layer
760	10 period, 300 Å / 300 Å , GaSb/AlSb superlattice	Same as 759

the indirect band edge of AlSb and 0.55 eV to the direct band edge of AlSb) between the two materials. The valence band offset in comparison has a value of 0.45 eV. A GaSb or AlSb single layer thickness of 300 Å was selected so that ionizing carriers could gain enough energy at high field conditions (E> 10^5 V/cm) to get out of the well. A total thickness of 0.6 μm for the superlattice layer enabled direct comparison with $Al_{0.04}Ga_{0.96}Sb$ devices which had multiplication regions of the same length.

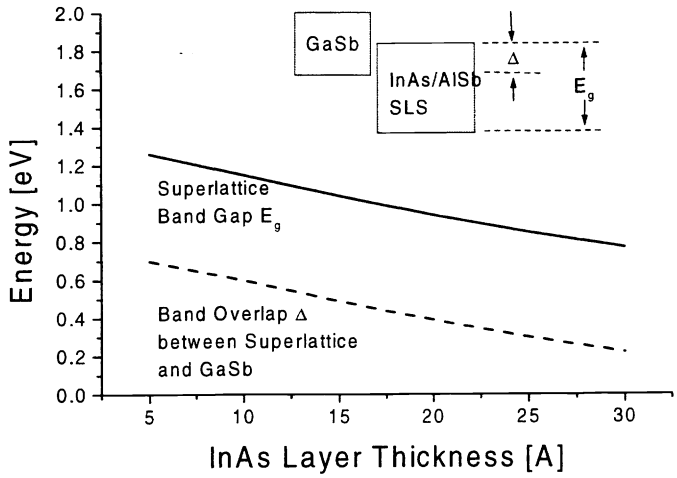

Figure 2. Calculated InAs/AlSb superlattice band gap energy and band overlap with GaSb as a function of superlattice period thickness.[14] The InAs and AlSb layer thicknesses were assumed to be equal.

The n^+ region of the abrupt pn junction was formed by using a short period InAs/AlSb superlattice, which was approximately lattice matched to GaSb when the InAs and AlSb layer thicknesses were kept the same. N-type doping ($n=1\times10^{18}/cm^3$) was achieved by selectively incorporating Si in the InAs layers.[15] The superlattice n-type layer has been previously reported by Miles and Chow et al.[2] in antimonide laser studies. The approach negated the need for a conventional Te dopant cell and provided separately tunable conduction and valence band edges. As shown in Fig. 2, the bandgap of the superlattice varied from 0.8 eV to 1.2 eV as the InAs layer thickness decreased from 27 Å to 10 Å. In this experiment, the InAs/AlSb superlattice bandgap was kept above the GaSb bandgap (0.72 eV) to ensure that long wavelength photons could reach the underlying substrate for pure electron injection during impact ionization measurements.[5] The superlattice design was also optimized in order to suppress tunneling current at the p^-n^+ interface and minimize the Schottky barrier at the surface. As shown in Table 1, these effect were explored by fabricating $Al_{0.04}Ga_{0.96}Sb$ multiplication layer devices with three different InAs/AlSb superlattice configurations. A graded InAs/AlSb superlattice incorporating three stages was found to have the best

dark current and contact characteristics (Section 4), hence this configuration was also used to fabricate devices with the superlattice multiplication layer.

3. GROWTH AND FABRICATION

The APD device structures were grown in a Perkin-Elmer 430 MBE system equipped with cracked As and Sb Sources. (100) GaSb wafers were used as substrates and etched prior to Indium bonding. Following oxide desorption under Sb over pressure, a 1 μm thick GaSb buffer was deposited at a substrate temperature of 520 °C. The buffer layer was heavily doped with Si and acted as the p^+ bottom contact to the device. The Si cell was shuttered off during growth of the unintentionally doped $Al_{0.04}Ga_{0.96}Sb$ or GaSb/AlSb superlattice multiplication layer. Samples were typically soaked in Sb for 10 to 30 seconds at each hetero-interface. A two dimensional growth front was ensured throughout the growth sequence by maintaining the 1×3 reflection high energy electron diffraction (RHEED) pattern characteristic of GaSb and AlSb reconstructed surface.

For growth of the selectively doped InAs/AlSb superlattice, the substrate temperature had to be lowered to prevent excessive As incorporation in the antimonide layers. The structural quality of the superlattice was significantly improved when the growth temperature was lowered to 420 °C, at which point the GaSb surface turns Sb rich and the RHEED pattern changes from 1×3 to 1×5. During growth of the InAs layer, the Si cell shutter was opened for n-type doping, and As flux was minimized by using the valved cracker while maintaining an As stabilized growth front. A 5 second Sb soak was applied between each InAs and AlSb interface to ensure an InSb like interface, which was known to produce material of superior quality.[16] RHEED patterns remained streaky even for short period superlattices and exhibited sharp 2×4 and 1×3 reconstructions for the InAs and AlSb layers, respectively.

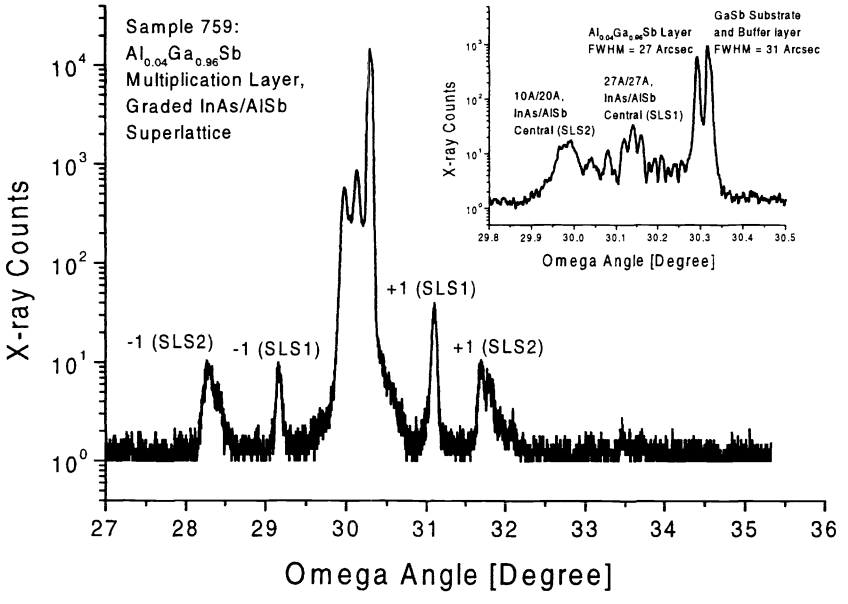

Figure 3. X-ray diffraction pattern of an APD structure fabricated from molecular beam epitaxy. The device had a 0.6 μm $Al_{0.04}Ga_{0.96}Sb$ multiplication region and three stages of InAs/AlSb superlattice (Sample 759). Inset shows a high resolution scan of the central region.

Fig. 3 shows the X-ray diffraction pattern obtained from sample 759, which had a bulk $Al_{0.04}Ga_{0.96}Sb$ multiplication layer followed by three stages of InAs/AlSb superlattice. Good structural quality was evidenced by the existence of satellite peaks from the 10 Å/20 Å and 27 Å/27 Å superlattice. The inset of Fig. 3 shows a high resolution scan of the central region. The $Al_{0.04}Ga_{0.96}Sb$ peak can be seen to clearly separate from the GaSb peak. The separation was used to accurately calibrate the composition of the multiplication layer. The $Al_{0.04}Ga_{0.96}Sb$ and GaSb buffer layer peaks had narrow and symmetric profiles with full width half maximums (FWHM) of about 30 arcsecs, which indicated that As incorporation in the antimonide layer was limited to below 0.1%.

Following MBE growth, standard photolithography was used to define the APD device mesa, which was circular in shape and ranged in size from 38 μm to 67 μm. Gold or Au:Ge was sputter deposited onto the sample for top contact whereas indium left over from MBE growth served as the back contact. The front metal layer thickness was kept thin at 50 Å for light transparency. Devices were also fabricated for direct injection of light into the semiconductor by employing a two step mask process. These mesas had a light sensitive circular opening surrounded by a ring of contact metal 2000 Å in thickness. Since the InAs/AlSb superlattice contained both arsenides and antimonides, standard wet etch recipes designed to work with either material could not be used. A satisfactory solution was found by using Cl_2 assisted dry etching, which was sometimes followed by a quick antimonide wet etch to anneal out the surface damage. Sulfur passivation[17] was also studied by soaking some samples in $(NH_4)_2S$ after the wet etch anneal. It was found that the additional wet etch step did not always improve dark current. Sulfur passivation did reduce surface leakage at low reverse biases, but the effect was much weakened near avalanche break down.

4. CURRENT-VOLTAGE ANALYSIS

A HP 4156 semiconductor parameter analyzer was used to probe the I-V characteristics of the APD devices. Fig. 4 shows the results from three devices with the same $Al_{0.04}Ga_{0.96}Sb$ multiplication layer and different InAs/AlSb superlattice configurations. The large variation in reverse current among these devices indicated that dark current suppression was closely related to the design of the InAs/AlSb superlattice. The effect can be understood by examining Fig. 2, which shows the calculated band overlap between GaSb and the InAs/AlSb superlattice as a function of the superlattice period. For samples with a 27 Å period superlattice, a high level of dark current was observed because the band overlap at the p^-n^+ junction was only 0.3 eV and the carriers can easily tunnel through the junction under reverse bias. In sample 757, the InAs well thickness was decreased to 10 Å and the electron energy level in the quantum well was pushed up, resulting in a higher superlattice conduction band edge and a greater band overlap (0.58 eV) at the p^-n^+ junction. The effect was reduced at the valence band edge because the relative shallowness of hole confinement, i.e. a change in the AlSb layer thickness induced a much smaller shift in the superlattice valence band. Note however that the exponential nature of the dark current in sample 757 indicated that it was still dominated by tunneling. Moreover, the shorter period superlattice resulted in a larger superlattice bandgap and a higher n-type Schottky barrier at the surface, as evidenced by the reduced forward conduction characteristics of Sample 757.

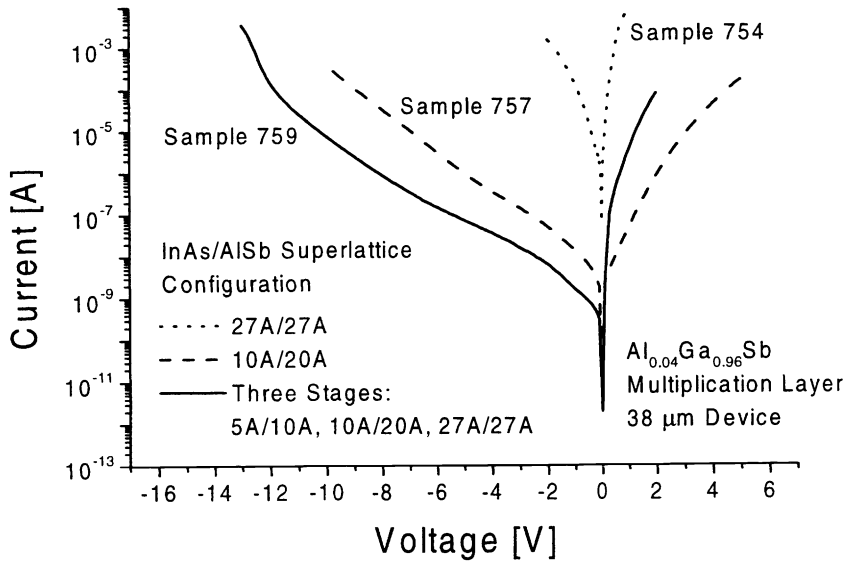

Figure 4. Current-Voltage characteristics of three APD devices with the same $Al_{0.04}Ga_{0.96}Sb$ multiplication layer and different InAs/AlSb n-type superlattices.

By employing a three stage InAs/AlSb superlattice, both the forward and reverse I-V characteristics were improved in sample 759. Compared to sample 757, the device was more conductive under forward bias due to the smaller band gap of the 27 Å/27 Å superlattice contact layer. The dark current was also further reduced as the InAs layer thickness was decreased to 5 Å near the p^-n^+ interface. The shorter period superlattice had a 0.7 eV band overlap with the $Al_{0.04}Ga_{0.96}Sb$ multiplication region and more effectively blocked the tunneling current. At low reverse bias, the dark current in sample 759 was still dominated by tunneling, but rapid current increase characteristic of avalanching action could be observed at about 12 V. A breakdown voltage of 13 V was consistently obtained and very close to the predicted value for an one sided abrupt pn junction (Section 2). The avalanche nature of the break down was confirmed by I-V characterization at liquid nitrogen temperature, where a lower avalanche onset voltage was observed due to reduced phonon scattering.[13]

The I-V characteristic of devices with the superlattice multiplication region is shown in Fig. 9(a). The device had the same graded InAs/AlSb superlattice structure as sample 759. The dark current in this device was an order of magnitude lower than in $Al_{0.04}Ga_{0.96}Sb$ devices due to the presence of AlSb barriers in the multiplication region. The larger bandgap of AlSb also contributed to a higher avalanche break down voltage of 18.5 V and more pronounced avalanching characteristics near break down.

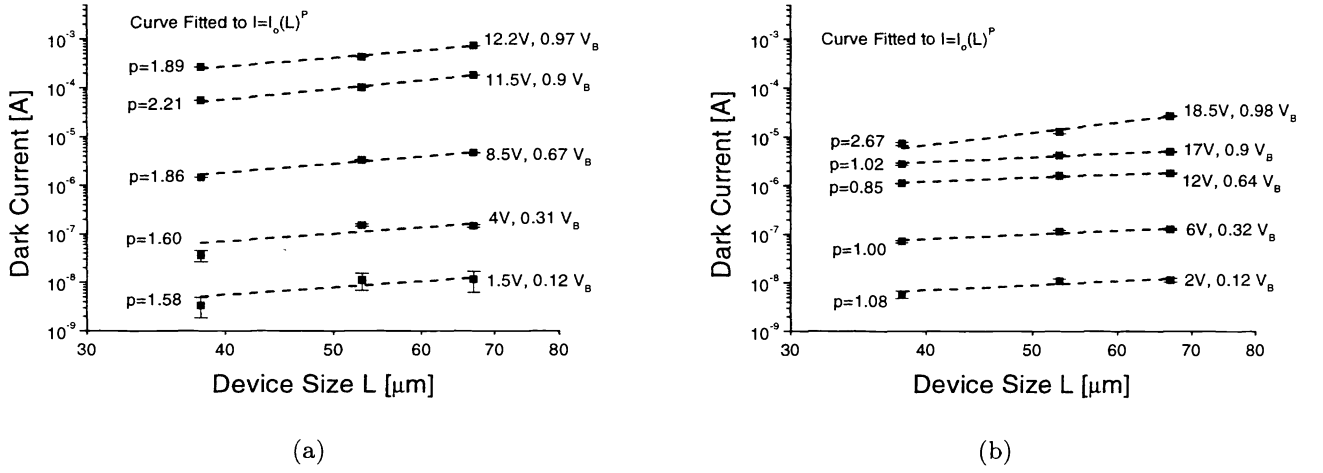

Figure 5. Dark current scaling with device size for APD's with (a) $Al_{0.04}Ga_{0.96}Sb$ multiplication layer and (b) GaSb/AlSb superlattice multiplication layer. The data is fitted to a power law $I=I_o(L)^P$, where L is the device size. The curve fit should yield p=2 for perfect scaling with device area and p=1 for perfect scaling with device perimeter.

To better understand the origin of the dark current, which was relatively high in devices with bulk $Al_{0.04}Ga_{0.96}Sb$ multiplication layers, current-voltage measurements from mesas of three different sizes were compared. In Fig. 5, the leakage current of $Al_{0.04}Ga_{0.96}Sb$ and superlattice devices were plotted against device mesa size at different voltages using a Log scale. The slope of the curve indicated whether the leakage current scaled with device area or perimeter, and provided a useful hint on the relative importance of bulk and surface leakage current. It can be seen that bulk leakage current was significant in $Al_{0.04}Ga_{0.96}Sb$ devices whereas surface leakage contributed to most of the dark current in the superlattice device until the onset of avalanche break down. This suggested that AlSb in the superlattice multiplication layer effectively blocked much of the tunneling dark current at low voltages. In contrast, the lower bandgap of $Al_{0.04}Ga_{0.96}Sb$ multiplication layer resulted in a relatively high level of bulk tunneling current.

5. PHOTO RESPONSE CHARACTERISTICS

A fiber optical set-up employing laser diodes was used to obtain the photo gain characteristics of the APD's. Light injection was achieved by butt coupling a single mode fiber (core diameter = 9 μm) to the top surface of the APD mesa. The signal was chopped at 10 kHz and picked up by a lock-in amplifier. Two laser diodes at wavelengths of

781 nm and 1645 nm were used to attempt front and back carrier injection so that electron and hole ionization rates could be measured.

5.1. Bulk $Al_{0.04}Ga_{0.96}Sb$ Devices

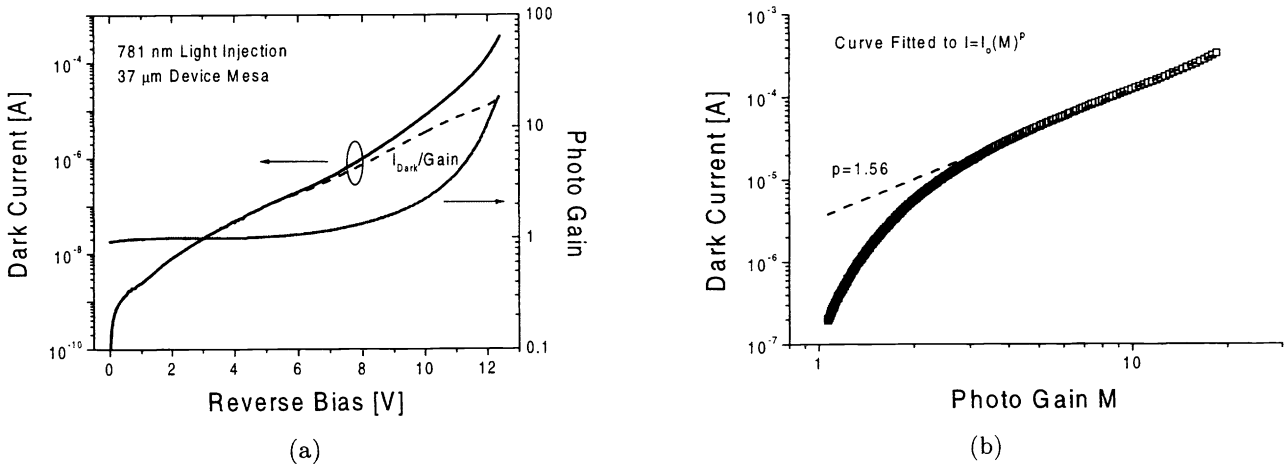

Figure 6. (a)Photo gain and dark current characteristics of APD's with $Al_{0.04}Ga_{0.96}Sb$ as the multiplication layer. The device had a three stage InAs/AlSb superlattice as the n^+ layer (Sample 759). The dashed line shows the un-multiplied dark current. (b)Device dark current plotted as a function of photo gain. The data is fitted to a power law $I=I_o(M)^p$ where p=1 for constant un-multiplied dark current.

Among the three samples with $Al_{0.04}Ga_{0.96}Sb$ multiplication layers, sample 759 had the best current-voltage characteristics and was used in the subsequent photo response characterization. The photo gain curve for 781 nm light is shown in Fig. 6(a) for a 38 μm device. A photo gain of 10 was obtained at a dark current density of 6 A/cm^2. Plotting the dark current in the avalanching region against the photo gain (Fig. 6(b)) revealed that the dark current increased faster than the photo current. The un-multiplied dark current was plotted in Fig. 6(a) and can be seen to increase exponentially with voltage, which indicated that the reverse leakage was due mostly to bulk tunneling, in agreement with findings from the I-V scaling study (Section 4).

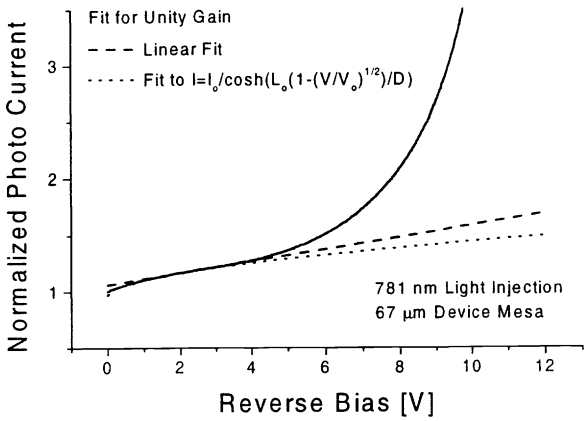

Figure 7. Photo response of an $Al_{0.04}Ga_{0.96}Sb$ APD without correction. The curve was fitted at low bias to correct for bias dependence of quantum efficiency.

The photo gain curve shown in Fig. 6(a) was corrected to account for changes in injection efficiency as the device bias was increased. Fig. 7 shows the actual measured photo current for 781 nm light at low reverse bias. The external quantum efficiency was estimated to be 16 % at zero bias and slowly rised as the bias was increased. An inflexion point in the photo gain curve can be seen at about 2 V. This effect could not be attributed to widening of the depletion region since 781 nm light was absorbed in the heavily doped n-type layer. In the absence of a convincing physical model, the photo gain at low bias was fitted to a straight line around the inflexion point, which was extracted to higher bias regions as unity gain. A similar but weaker effect was also observed for 1645 nm light, which yielded an external quantum efficiency of 10 % at zero bias. For consistency, linear fitting was again used to correct for unity gain instead of the more complicated depletion widening model.[18]

When the APD device was illuminated by 1645 nm laser light, the photon energy was just below the band gap of the $Al_{0.04}Ga_{0.96}Sb$ multiplication layer, resulting in absorption in the underlying p-type GaSb layer and pure electron injection. Hole injection was achieved by using 781 nm light because the more energetic photons were absorbed in the higher bandgap n-type material. Fig. 8(a) shows the corrected photo gain curves for 781 nm and 1645 nm light from the same junction. These curves were highly reproducible and independent of light intensity, device size, and injection geometry. The electron and hole impact ionization rates can be derived from these curves by using the formulas[5]:

$$k_n(E) = E\frac{1}{M_n(V)M_p(V)}\frac{dM_n(V)}{dV} \tag{1}$$

$$k_p(E) = E(\frac{1}{M_p(V)}\frac{dM_p(V)}{dV} - \frac{1}{M_n(V)}\frac{dM_n(V)}{dV}) + k_n(E) \tag{2}$$

where k_n and k_p are the electron and hole impact ionization rates, $M_n(V)$ and $M_p(V)$ the photo gain at bias V for electron and hole injection, and E the maximum electric field in the abrupt pn junction at bias V.

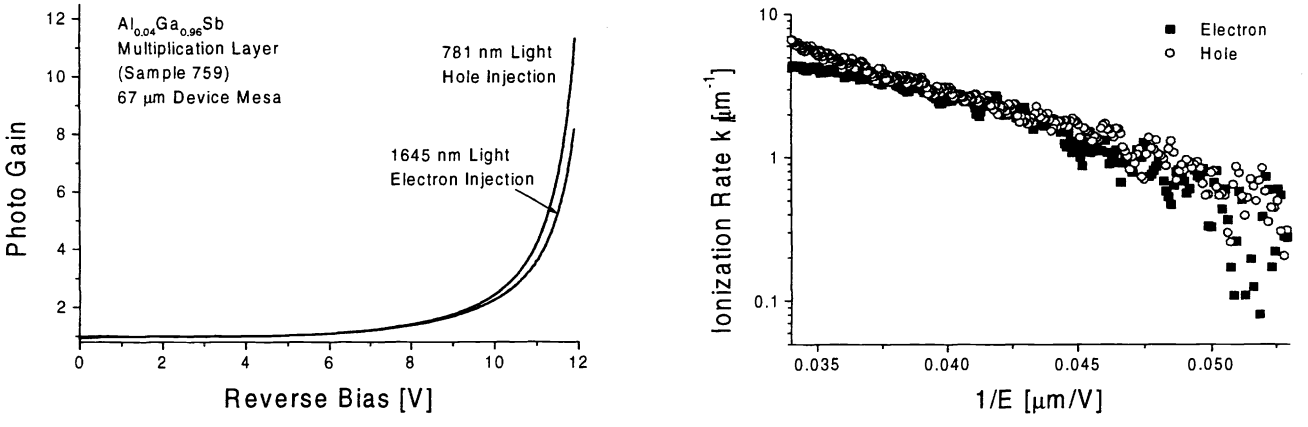

(a) (b)

Figure 8. (a)Photo gain curves for hole and electron injection using 781 nm and 1645 nm light. (b)Calculated hole and electron impact ionization rates in $Al_{0.04}Ga_{0.96}Sb$. The device was assumed to have an abrupt pn junction.

The calculated ionization rates are shown in Fig. 8(b) and can be seen to deviate from the Shockley model[19] (straight line in $\log(K_n)$ vs. 1/E plot) at high and low electric fields. This may be because pure electron injection was not achieved due to Franz-keldysh absorption of 1645 nm photons in the $Al_{0.04}Ga_{0.96}Sb$ layer. Another possibility is that quantum efficiency increased more rapidly at higher bias and the straight line fit for unity gain was not adequate. This was evidenced by the fact that the two curves in Fig. 8(a) lied on top of each other before reaching a nominal photo gain of 2. The observed gain before this point may be due to an increase in quantum efficiency.

Note however that the photo gain curves were consistent with enhancement of hole impact ionization since higher gains were always obtained for hole injection. A better model for the bias dependence of quantum efficiency would be needed to extract ionization rates from these data.

5.2. Superlattice Devices

Photo response measurements were also performed on APD's with superlattice multiplication regions. The external quantum efficiencies for 781 nm and 1645 nm light were 20 per cent and 5 per cent at unity gain, respectively. The 1645 nm light was absorbed in the multiplication region due to the presence of GaSb layers, hence only hole injection was achieved. Within experimental error, the photo gain curves for light at the two wavelengths were the same. Fig. 9 shows the 1645 nm photo gain characteristics of a 37 μm device and the associated dark current. Gain factors as high as 300 were obtained in some devices. At a gain factor of 10, the dark current for the 37 μm device was 10 μA, which was an order of magnitude lower than in bulk $Al_{0.04}Ga_{0.96}Sb$ devices, and comparable to InGaAs/InAlAs superlattice APD's of similar design.[12] The dark current was plotted against photo gain in Fig. 9(b). Unlike its bulk $Al_{0.04}Ga_{0.96}Sb$ counterpart (Fig. 8(b)), the dark current in the superlattice device increased slower than the photo current. In fact, the un-multiplied dark current stayed constant or decreased with voltage in the superlattice device. This indicated that much of the dark current was not multiplied and must be due to surface leakage. The result was consistent with findings from dark current scaling studies in Section 4. Thus the observed dark current characteristics of the superlattice device did not represent its fundamental limit. With better processing and passivation technique, the surface leakage can be readily reduced and device performance further improved.

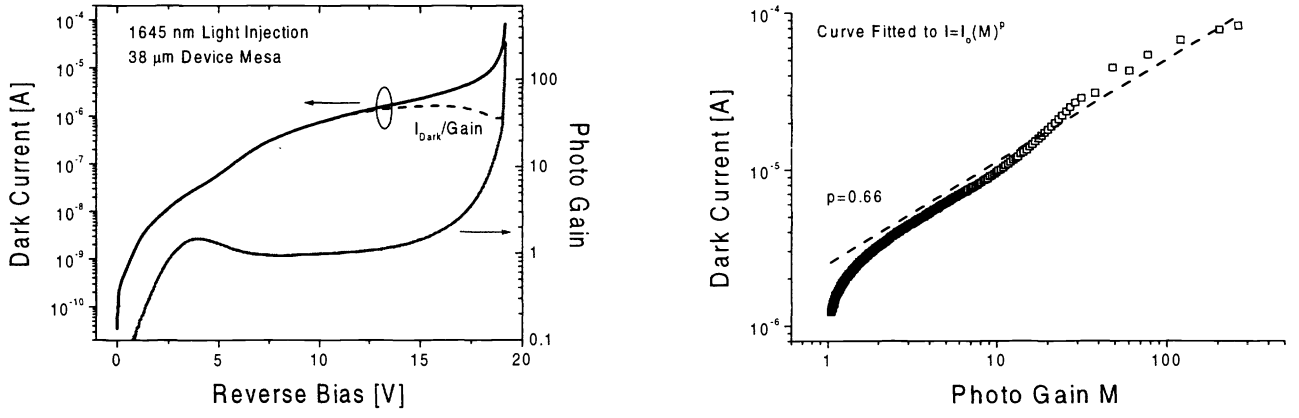

(a) (b)

Figure 9. (a)Photo gain and dark current characteristics of APD's with a 10 period, 300 Å/300 Å, GaSb/AlSb multiplication layer. The dashed line shows the un-multiplied dark current. (b)Device dark current plotted as a function of photo gain. The data is fitted to a power law $I=I_o(M)^p$, which should yield p=1 for constant un-multiplied dark current.

It should be noted that the superlattice photo gain curve differed significantly from its bulk $Al_{0.04}Ga_{0.96}Sb$ counterpart at low reverse bias. The superlattice collection efficiency was strongly dependent on device bias at low voltages due to the presence of AlSb barriers in the multiplication region. A bias as high as 10 V was needed to overcome the barrier and achieve unity gain. The bias needed to sweep out the photo generated carriers was also dependent on the incident light intensity. As shown in Fig. 10, at greater input light intensity, a higher reverse bias was need to achieve the same quantum efficiency and unity gain. We attribute this effect to carrier trapping in the quantum wells in the multiplication region,[20] which tended to screen the applied electric field. A small bump was also observed in the photo gain curve at low levels of light injection. Work is still in progress to understand this photo induced negative resistance effect.

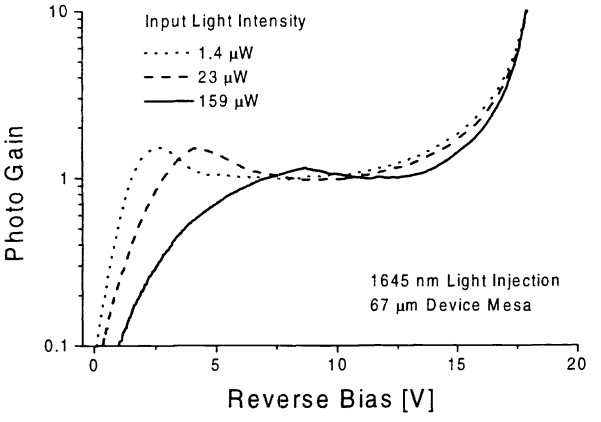

Figure 10. Photo response of the GaSb/AlSb superlattice APD at different light intensity levels. The data was obtained by using a 1645 nm laser light. Similar results were obtained from the 781 nm light source.

6. CONCLUSION

We have demonstrated that antimonide APD's with bulk or superlattice multiplication regions can be fabricated from molecular beam epitaxy. The dominant mechanism of dark current generation in bulk $Al_{0.04}Ga_{0.96}Sb$ devices was identified as tunneling at the multiplication to n-type layer interface. The dark current was henceforth improved by using a three-stage n-type superlattice. Photo gain curves at two different wavelengths were obtained for bulk $Al_{0.04}Ga_{0.96}Sb$ devices and yielded results consistent with hole impact ionization enhancement. APD devices with GaSb/AlSb superlattice multiplication layers exhibited lower dark currents and more pronounced avalanche characteristics due to the presence of large band gap material in the multiplication region. The superlattice structure is promising since the device dark current was found to be limited by surface leakage and can be readily improved by using better processing and passivation.

ACKNOWLEDGMENTS

The authors would like to thank A. T. Hunter and D. H. Chow of Hughes Research Lab for helpful discussions of antimonide growth and APD characterization. We also gratefully acknowledge the support of the Defense Advanced Research Projects Agency monitored by the Army Research Laboratory under contract number DAAL 01-97-K-0121.

REFERENCES

1. R. Q. Yang and S. S. Pei, "Novel type-II quantum cascade lasers," *J. Appl. Phys.* **79**, pp. 8197-8203, 1996.
2. R. H. Miles, D. H. Chow, T. C. Hasenberg, A. R. Kost and Y-H. Zhang, "Mid-infrared laser diodes based on GaInSb/InAs and InAs/AlSb superlattices," *Appl. Phys. Lett.* **67**, pp. 3700-3702, 1995.
3. D. L. Smith and C. Mailhiot, "Proposal for strained type II superlattice infrared detectors," *J. Appl. Phys.* **62**, pp. 2545-2548, 1987.
4. F. Osaka, T. Mikawa, T. Kaneda, "Impact ionization coefficients of electrons and holes in (100)-oriented $Ga_xIn_{1-x}As_yP_{1-y}$," *IEEE J. Quantum Electron.* **OE-21**, pp. 1326-1338, 1985.
5. G. E. Stillman and C. M. Wolfe, in *Semiconductors and Semimetals* **Volume 12**, edited by R. K. Willard and A. C. Beer, Academic, New York, 1977.
6. O. Hildebrand, W. Kuebart, K. W. Benz, and M. H. Pilkuhn, "$Ga_{1-x}Al_xSb$ avalanche photodiodes: resonant impact ionization with very high ratio of ionization coefficients," *IEEE J. Quantum Electron.* **OE-17**, pp. 284-288, 1981.
7. L. Gouskov, B. Orsal, M. Perotin, M. Karim, A. Sabir, P. Coudray, S. Kibeya, and H. Luquet, "Impact ionization in $Ga_{1-x}Al_xSb$,", *Appl. Phys. Lett.* **60**, pp. 3030-3032, 1992.

8. H. Kuwatsuka, T. Mikawa, S. Miura, N. Yasuoka, Y. Kito, T. Tanahashi, and O. Wada, "Measurement of the impact ionization rates in $Al_{0.06}Ga_{0.94}Sb$," *Appl. Phys. Lett.* **57**, pp. 249-251, 1990.
9. Y. Jiang, M. C. Teich, and W. I. Wang, "Hole impact ionization enhancement in $Al_xGa_{1-x}Sb$," *J. Appl. Phys.* **67**, pp. 2488-2493, 1990.
10. G. F. Williams, F. Capasso, and W. T. Tsang, "The graded bandgap multilayer avalanche photodiode: a new low noise detector," *IEEE Elect. Device. Lett.* **3**, pp. 71-73, 1982.
11. F. Cappasso, W. T. Tsang, A. L. Hutchinson, and G. F. Williams, "Enhancement of electron impact ionization in a superlattice: a new avalanche photodiode with a large ionization rate ratio," *Appl. Phys. Lett.* **40**, pp. 38-40, 1982.
12. T. Kagawa, Y. Kawamura, H. Asai, M. Naganuma, and O. Mikami, "Impact ionization rates in an InGaAs/InAlAs superlattice," *Appl. Phys. Lett.* **66**, pp. 993-995, 1989.
13. S. M. Sze, *Physics of Semiconductor Devices*, John Wiley Sons. Inc., 1981
14. J. N. Schulman and R. H. Miles, unpublished.
15. D. H. Chow, Y. H. Zhang, R. H. Miles, and H. L. Dunlap, "Structural and transport properties of InAs/AlSb superlattices," *J. Cryst. Growth.* **150**, pp. 879-882, 1995.
16. G. Tuttle, H. Kroemer, and J. H. English, "Effects of interface layer sequencing on the transport properties of InAs/AlSb quantum wells - evidence for antisite donors at the InAs/AlSb interface," *J. Appl. Phys.* **67**, pp. 3032-3037, 1990.
17. M. Perotin, P. Coudray, A. Etcheberry, L. Gouskov, C. Debiemme-Chouvy, and H. Luquet, "Improvement of dark current of Ga(Al)Sb mesa diodes using $(NH_4)_2S$," *Materials Science and Engineering* **B28**, pp. 374-378, 1994.
18. M. H. Woods, W. C. Johnson, and M. A. Lampert, "Use of a Schottky barrier to measure impact ionization coefficients in semiconductors," *Solid State Electron.* **16**, pp. 381-394, 1973.
19. W. Shockley, "Problems related to pn junction in Si," *Solid State Electron.* **2**, pp. 35-67, 1961.
20. R.E. Cavicchi, D. V. Lang, D. Gerhsoni, A. M. Sergent, H. Temkin, and M. B. Panish, "Sequential screening layers in a photoexcited $In_{1-x}Ga_xAs$/InP Superlattice," *Phys. Rev. B* **38**, pp. 13474-13477, 1988.